Specific thylakoid protein phosphorylations are prerequisites for overwintering of Norway spruce (*Picea abies*) photosynthesis

Steffen Grebe[a,1], Andrea Trotta[a,b,1], Azfar Ali Bajwa[a], Ilaria Mancini[a], Pushan Bag[c], Stefan Jansson[c], Mikko Tikkanen[a], and Eva-Mari Aro[a,2]

[a]Molecular Plant Biology, University of Turku, FI-20520 Turku, Finland; [b]Institute of Biosciences and Bioresources, National Research Council of Italy, 50019 Sesto Fiorentino (Firenze), Italy; and [c]Umeå Plant Science Centre, Department of Plant Physiology, Umeå University, 901 87 Umeå, Sweden

This contribution is part of the special series of Inaugural Articles by members of the National Academy of Sciences elected in 2018.

Contributed by Eva-Mari Aro, June 1, 2020 (sent for review March 4, 2020; reviewed by Krishna K. Niyogi and Jean-David Rochaix)

Coping of evergreen conifers in boreal forests with freezing temperatures on bright winter days puts the photosynthetic machinery in great risk of oxidative damage. To survive harsh winter conditions, conifers have evolved a unique but poorly characterized photoprotection mechanism, a sustained form of nonphotochemical quenching (sustained NPQ). Here we focused on functional properties and underlying molecular mechanisms related to the development of sustained NPQ in Norway spruce (*Picea abies*). Data were collected during 4 consecutive years (2016 to 2019) from trees growing in sun and shade habitats. When day temperatures dropped below −4 °C, the specific N-terminally triply phosphorylated LHCB1 isoform (3p-LHCII) and phosphorylated PSBS (p-PSBS) could be detected in the thylakoid membrane. Development of sustained NPQ coincided with the highest level of 3p-LHCII and p-PSBS, occurring after prolonged coincidence of bright winter days and temperatures close to −10 °C. Artificial induction of both the sustained NPQ and recovery from naturally induced sustained NPQ provided information on differential dynamics and light-dependence of 3p-LHCII and p-PSBS accumulation as prerequisites for sustained NPQ. Data obtained collectively suggest three components related to sustained NPQ in spruce: 1) Freezing temperatures induce 3p-LHCII accumulation independently of light, which is suggested to initiate destacking of appressed thylakoid membranes due to increased electrostatic repulsion of adjacent membranes; 2) p-PSBS accumulation is both light- and temperature-dependent and closely linked to the initiation of sustained NPQ, which 3) in concert with PSII photoinhibition, is suggested to trigger sustained NPQ in spruce.

Picea abies | phosphorylation | PSBS | LHCII | sustained NPQ

Molecular mechanisms associated with winter acclimation of evergreen plants comprise a number of different processes, like biosynthesis of osmolytes to protect against freezing damages, and changes in membrane lipid and fatty acid composition to modulate the fluidity and other properties of intracellular membranes (reviewed in ref. 1). These acclimation steps are typical for chloroplasts as well, yet they do not provide a solution for a unique property of evergreen plants, the coping with high light intensities under freezing temperatures, which potentially leads to severe photooxidative damages. Different solutions to avoid extensive photodamage have evolved among evergreens (1), all closely interlinked with regulation and functionality of the photosynthetic apparatus in chloroplasts (2). In conifers, the protection against photodamage is largely achieved by regulatory nonphotochemical quenching (NPQ) of excess light energy. However, under freezing temperatures and bright light, a specific long-lasting energy dissipation state, historically assigned as sustained NPQ (1), is induced.

Regulatory NPQ, which harmlessly dissipates excess absorbed light energy as heat in response to environmental cues, is typical for all plant species and carried out by several different mechanisms (3–5). Distinct components of regulatory NPQ have been defined by investigation of the relaxation kinetics of chlorophyll fluorescence in darkness after previous exposure of leaves to high light. The components include the fast relaxing qE (energy-dependent quenching), more slowly relaxing qZ (zeaxanthin-dependent quenching) and qH (plastid lipocalin-dependent quenching), as well as a very slowly relaxing qI (photoinhibitory quenching) (for reviews, see refs. 5 and 6), the latter component in fact requiring low light for full recovery via the photosystem II (PSII) repair cycle (7, 8). The regulatory NPQ components, qE and qZ, are controlled by formation of thylakoid transmembrane ΔpH in the light. qE is linked to protonation of the PSBS protein and aggregation of light-harvesting complex II (LHCII) proteins, while qZ is linked to the conversion of violaxanthin to zeaxanthin, and the components of the novel qH mechanism are only emerging (9).

In evergreen conifers, like Norway spruce (hereafter spruce), besides capable of dynamic regulatory NPQ, the sustained NPQ

Significance

During overwintering, evergreen conifers of boreal forests must cope with freezing temperatures and high light intensities that often occur simultaneously and expose the photosynthetic apparatus to oxidative damage. To mitigate damage, conifers have developed a specific photoprotection mechanism, called sustained nonphotochemical quenching (sustained NPQ). Here we provide evidence for involvement of unique post-translational phosphorylations of thylakoid proteins in sustained NPQ of spruce. The triply phosphorylated LHCB1 isoform and phospho-PSBS protein appear as prerequisites for development of sustained NPQ that safely dissipate absorbed light energy as heat. While the induction of Lhcb1 triple phosphorylation requires only freezing temperatures, the triggering of sustained NPQ is additionally dependent on light-induced PSBS phosphorylation, likely in concert with limited photoinhibition of photosystem II.

Author contributions: S.G., A.T., P.B., S.J., M.T., and E.-M.A. designed research; S.G., A.T., A.A.B., and I.M. performed research; E.-M.A. contributed new reagents/analytic tools; S.G., A.T., A.A.B., P.B., S.J., and E.-M.A. analyzed data; and S.G., A.T., M.T., and E.-M.A. wrote the paper.

Reviewers: K.K.N., University of California, Berkeley; and J.-D.R., University of Geneva.

The authors declare no competing interest.

Data deposition: The mass spectrometry proteomics data have been deposited to the ProteomeXchange Consortium via the PRIDE partner repository (dataset identifier PXD018941; DOI: 10.6019/PXD018941.

[1]S.G. and A.T. contributed equally to this work.

[2]To whom correspondence may be addressed. Email: evaaro@utu.fi.

This article contains supporting information online at https://www.pnas.org/lookup/suppl/doi:10.1073/pnas.2004165117/-/DCSupplemental.

First published July 20, 2020.

develops during winter provided the temperature drops well below 0 °C and daily illumination is high (1, 10). Sustained NPQ is demonstrated as a decrease of the maximal photochemical quantum yield of PSII (Fv/Fm), which relaxes extremely slowly. Dissipation of excess light energy via sustained NPQ prevents the accumulation of harmful reactive oxygen species in freezing temperatures by effectively diverting the absorbed light energy toward dissipation as heat. The molecular components and mechanisms specifically characterizing the development and relaxation of sustained NPQ during the winter period have remained mostly unknown, yet the phenomenon itself and consequences of sustained NPQ on thylakoid organization have been extensively investigated (see reviews in refs. 1 and 10).

A direct correlation has been reported between high amounts of zeaxanthin and sustained NPQ during the winter acclimation of conifers (11–13). However, more recent studies seem to indicate that zeaxanthin plays a more indirect role and is not directly involved in NPQ mechanisms (14, 15). From another perspective, the chloroplasts of spruce and other conifer species appear to undergo distinct ultrastructural changes during the winter period, with possible connection to the development of sustained NPQ. Such changes include a severe loss of grana stacking, which in turn would allow spillover quenching of excess light energy via PSI (1, 16–18). Grana stacking is influenced by the interaction of the stroma exposed N termini of both the LHCII and PSII proteins of the opposite thylakoids in grana (19, 20). Reversible phosphorylation of their N-terminal Thr residues by thylakoid kinases STN7 and STN8 (21, 22) is known to control the size of the partition gap between opposite thylakoid layers (23) and also regulates the state transitions (21), as well as other associations of LHCII with PSII and PSI (24–28). However, the spruce thylakoid phosphoproteins and their dynamics have remained poorly characterized.

Here we investigated if overwintering of spruce involves still unknown dynamics of thylakoid protein phosphorylations that would serve as molecular mechanisms for development of sustained NPQ. We started with an ecophysiological approach by collecting spruce branches from their natural habitat during 4 consecutive years and complemented these experiments with artificial light and temperature treatments of spruce. Needles were subjected to in-depth fluorescence and absorption analyses to estimate the photochemical and nonphotochemical energy dissipation modes and capacities, as well as to parallel proteome investigations of the thylakoid protein complexes (29) and

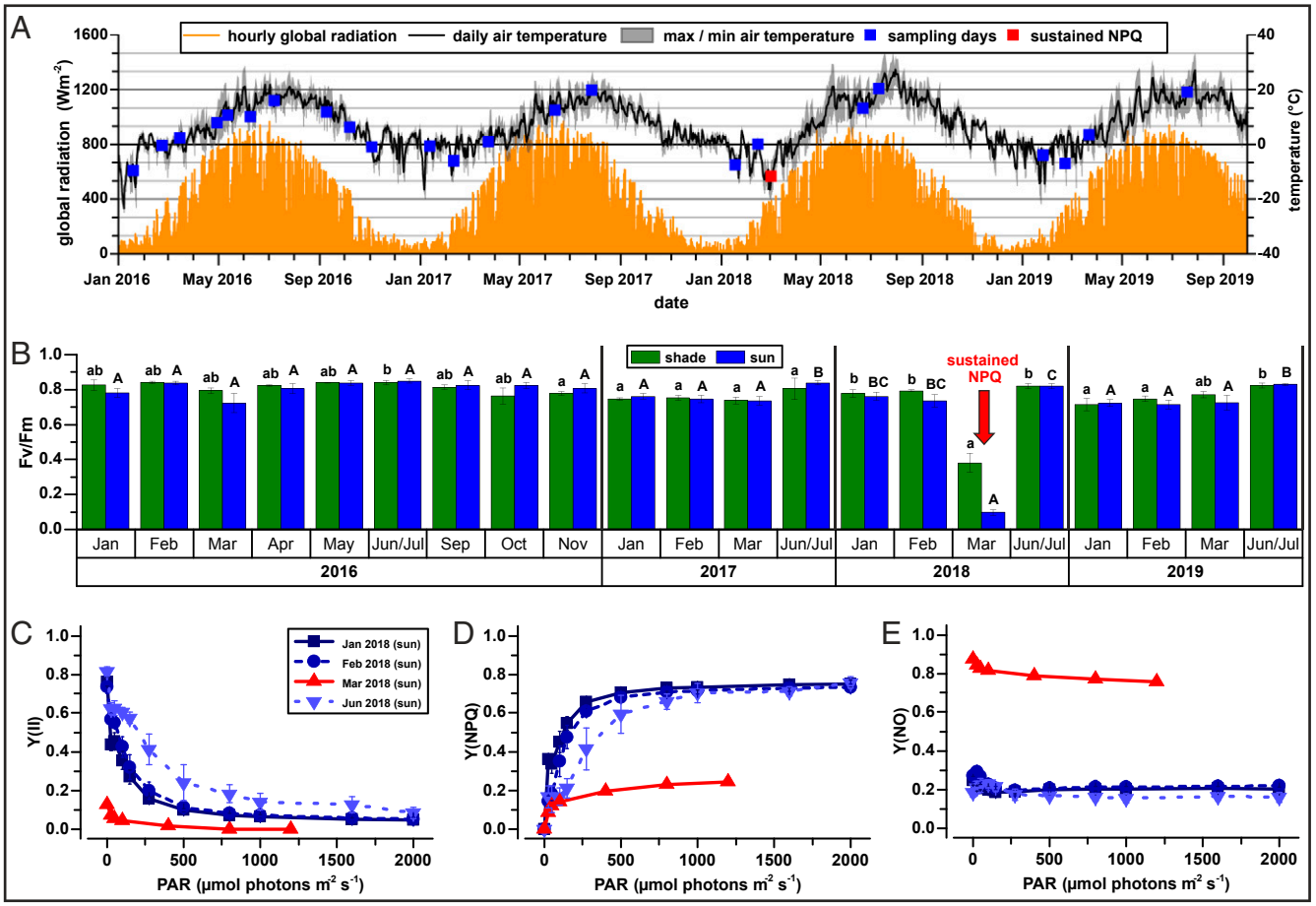

Fig. 1. Seasonal weather data and changes in spruce PSII fluorescence parameters. (*A*) Average hourly global radiation (W m^{-2}) and daily temperature (°C) during sampling period from 2016 to 2019 in Turku, Southern Finland. Sampling days are marked with blue squares, while sustained NPQ conditions are indicated with a red square. (*B*) Maximum quantum yield of PSII photochemistry (Fv/Fm) from all sampling points 2016 to 2019 of shade (green bars) and sun (blue bars) needles. Average of three biological replicates with SDs are shown. Red arrow indicates observation of sustained NPQ in Mar 2018. Letters (shade = lowercase, sun = uppercase) represent statistically significant groups, which were individually tested for each year and habitat: Years 2016 and 2017 (Welch's ANOVA, Games–Howell, $P < 0.05$) and years 2018 and 2019 (one-way ANOVA, Bonferroni, $P < 0.05$.). (*C–E*) PSII yield parameters from light-curve experiments of sun needles of 2018: (*C*) Effective quantum yield of PSII photochemistry, Y(II); (*D*) quantum yield of regulatory nonphotochemical quenching, Y(NPQ); and (*E*) quantum yield of nonregulatory energy dissipation, Y(NO). Average of three biological replicates with SDs are shown, except for sustained NPQ samples from March 2018 (red). Here only the least quenched (highest Fv/Fm) replicate is shown (*SI Appendix*).

protein phosphorylations. It is suggested that unique and dynamic phosphorylations of the LHCB1_A and PSBS proteins provide structural and functional adjustments in the thylakoid membrane that, together with limited PSII photoinhibition, contribute to stepwise development of sustained NPQ in spruce.

Results

Strategy of Sample Collection from Natural Sun and Shade Environments. To shed light on the mechanisms involved in the development of sustained NPQ in spruce, we collected spruce samples from natural environments and focused on thylakoid functional properties and protein changes during winter acclimation. The sampling points of spruce needles during the 4 consecutive years, together with temperature and light-intensity recordings, are shown in Fig. 1*A*. Spruce branches from sun- and shade-exposed trees in southern Finland were harvested and transported to the laboratory. The needles were dark-acclimated and probed via in vivo chlorophyll fluorescence and P700 difference absorption at room temperature. During 2016, needles were collected once a month all year round. As no major decline in Fv/Fm (Fig. 1*B*) was observed during 2016, the sampling of needles in the following 3 y (2017 to 2019) was focused on winter/early spring, with sustained NPQ eventually occurring in March 2018, and on summer months as typical nonsustained NPQ conditions (Fig. 1*B*).

Seasonal Variations in Capacity of Photochemistry and NPQ. Sustained NPQ was observed during the 4 y monitored only in March 2018 (Fig. 1*A*, red square), when freezing temperatures and high light intensities occurred simultaneously. In these conditions, Fv/Fm was strongly reduced to 0.38 and 0.10 in shade and sun needles, respectively (Fig. 1*B*). In other winter and early spring sampling points, Fv/Fm was reduced on average only to 0.77 and 0.75 compared to 0.82 and 0.84 in summer sampling points of shade and sun needles, respectively. In the winter and early spring experiments we cannot, however, fully exclude a putative minor relaxation of sustained NPQ during the transportation and prehandling of the needles. Nevertheless, the light curve experiments with increasing actinic light intensities, monitored from 2017 to 2019 needles (Fig. 1 *C*–*E* and *SI Appendix*, Figs. S1 and S2), revealed a strong reduction in effective quantum yield of PSII photochemistry, Y(II), only in March 2018 samples, indicative of sustained NPQ (Fig. 1*C*). In addition, the quantum yield of regulatory NPQ, Y(NPQ), was drastically lowered (Fig. 1*D*), while the quantum yield of nonregulatory energy dissipation, Y(NO), which also reflects sustained NPQ because of not relaxing during dark incubation, was strongly elevated in March 2018 needles in comparison to other winter samples (Fig. 1*E*). Conversely, in nonquenched winter and spring needles of all years, Y(II) was only slightly reduced while Y(NPQ) was elevated at low actinic light intensities compared to summer conditions. Noteworthy, and contrary to what would have been expected, the maximum Y(NPQ) obtained at high actinic light intensities in winter samples was as high as in summer samples (Fig. 1 *C*–*E* and *SI Appendix*, Fig. S1). In general, the shade needles showed fewer differences between winter/spring and summer conditions as compared to the sun needles (*SI Appendix*, Fig. S1).

During sustained NPQ conditions (March 2018 samples), PSI yield parameters were also strongly affected (*SI Appendix*, Fig. S2). At low actinic light intensities, the severely decreased PSII activity resulted in high donor side limitation of PSI, Y(ND). Consequently, the effective quantum yield of PSI photochemistry, Y(I), was strongly reduced. At higher actinic light intensities, a slightly higher acceptor side limitation of PSI, Y(NA), was observed. In all other winter and spring samples lacking the sustained NPQ, only minor variations in the PSI yield parameters between the sun and shade needles could be observed without any clear trend (*SI Appendix*, Fig. S2).

2016 Year-Round Investigation of Thylakoid Protein Complexes. In parallel to the in vivo PSII and PSI functional measurements described above, spruce needles were subjected to isolation of thylakoid membranes immediately after collection from their natural habitats. The samples collected once a month in 2016 were then analyzed, side by side, with large-pore blue-native (lpBN)/PAGE for comparison of the composition of photosynthetic protein complexes. Conspicuous seasonal temperature and light variations were also typical in 2016 (Fig. 1*A*), despite the absence of sustained NPQ (Fig. 1*B*), but no clear seasonal trends in the composition of thylakoid pigment protein complexes were evident (*SI Appendix*, Fig. S3). This observation, together with mostly minor differences in the capacity of photochemistry in nonsustained NPQ winter samples (Fig. 1*C*), provided evidence for robustness of spruce photosynthetic apparatus but also raised a question if differences in thylakoid protein complexes and their subunits are limited only to sustained NPQ condition.

Search for Thylakoid Phosphoproteins Related to Sustained NPQ. Next, we focused on the two most extreme types of seasonal samples, the sustained NPQ samples of March 2018 and the summer samples of June 2018, and subjected them to in-depth search for thylakoid phosphoproteins and their occurrence in different pigment protein complexes. To this end, the 1D lpBN/PAGE strip was loaded on top of the SDS-PAGE, run in second dimension and stained with Sypro protein stain (Fig. 2*A*) and ProQ phosphoprotein stain (Fig. 2*B*). Sypro protein stain revealed the typical pattern of spruce photosynthetic complexes and their subunits (29) (*SI Appendix*, Fig. S4), yet clear differences could be spotted between the sustained NPQ and summer samples. In summer, LHCII gave rise to three distinct canonical protein bands composed of LHCB1 (canonical bands 1 and 2) and LHCB2 (canonical band 3) isoforms (for nomenclature see Fig. 2*C*), which were visible in LHCII–PSII supercomplexes, LHCII trimers, and monomers. Intriguingly, in sustained NPQ needles, in addition to the three canonical LHCII protein bands, a doublet of higher molecular mass bands was also visible (Fig. 2*A*). Moreover, as revealed by the ProQ phosphoprotein stain, these particular LHCII polypeptides were highly phosphorylated in sustained NPQ needles, opposite to that of the summer samples (marked as 3p-LHCII in Fig. 2*B*). Besides the appearance of the new dominant phospho-LHCII proteins (3p-LHCII) in sustained NPQ needles, another phosphospot missing from summer needles was also visible in the free protein range (identified as p-PSBS, see below) (Fig. 2*B*). Furthermore, accumulation of CP43-less PSII subcomplex (RC-CP47) was evident only in sustained NPQ samples. This complex is a typical intermediate during the PSII repair cycle (8) and a clear indication of PSII photoinhibition during sustained NPQ conditions. It also appeared that the phosphorylated form of PSII protein D1 (p-D1) comigrates in spruce with the canonical LHCII bands (Fig. 2 *A* and *B* and *SI Appendix*, Fig. S4), different from that in angiosperms.

MS/MS Analysis of Phosphorylated LHCII and PSBS Proteins. The three canonical LHCII trimer bands (Fig. 2*C*), as well as the higher-molecular-mass phosphoproteins present particularly in the winter samples (marked with red arrows in the 2D-lpBN/SDS-PAGE gels of Fig. 2 *A* and *B*), were subjected to mass spectrometry analysis (MS/MS) and identified as LHCB1/2 isoforms and PSBS (Fig. 2 *C* and *D* and Dataset S1). It is noteworthy that in spruce and other Pinaceae, the trimeric LHCII consists only of LHCB1 and LHCB2 subunits, while LHCB3 has been lost (29, 30). The N-terminal region of LHCB1/2 isoforms generally harbors multiple Ser and Thr phosphosites, which are conserved throughout the evolution of land plants (31). Additionally, two distinct LHCB1 isoforms, LHCB1_A and LHCB1_B, were identified in spruce [previously also in pine (32)], with the

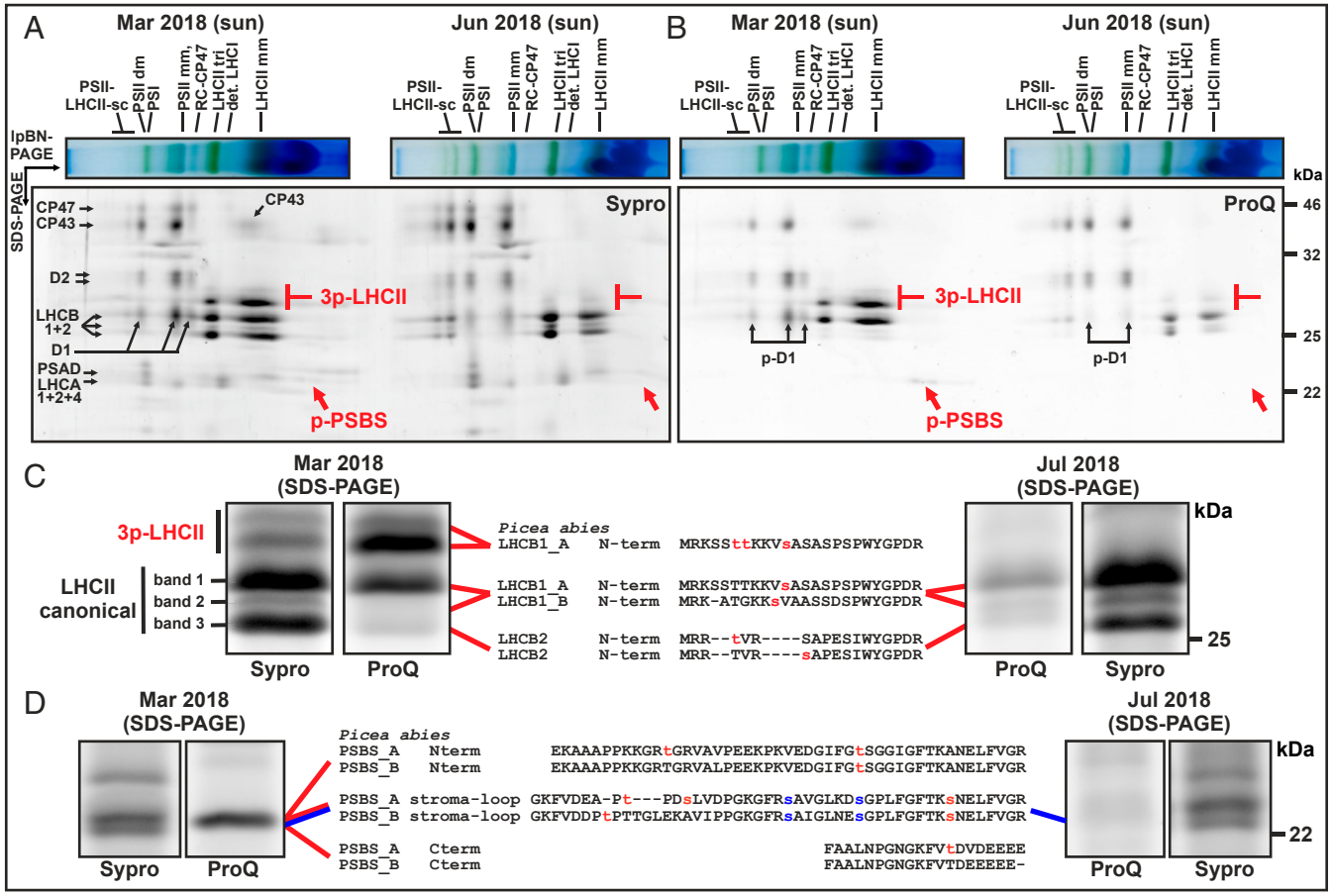

Fig. 2. Thylakoid protein composition of spruce needles in sustained NPQ condition in comparison to summer conditions and identification of LHCII and PSBS phosphorylations. (*A* and *B*) Two-dimensional lpBN/SDS-PAGE of isolated thylakoids of sustained NPQ needles from March 2018 (*Left*) and June 2018 (*Right*) of sun needles stained with (*A*) total protein stain (Sypro) and (*B*) phosphoprotein stain (ProQ). Red arrows indicate phosphoproteins in spruce thylakoids, 3p-LHCII doublet, and p-PSBS spots. lpBN gel was loaded on equal chlorophyll basis (5 μg). Only the molecular mass region between 46 and 17 kDa in second dimension is shown. The full molecular mass range gel is shown in *SI Appendix*, Fig. S4. det., detached; dm, dimer; mm, monomer; sc, supercomplex; tri, trimer. (*C*) Identified N-terminal phosphopeptides of LHCII proteins in sun needles of spruce. Different phosphopeptides of LHCB1_A, LHCB1_B and LHCB2 in bands of LHCII from thylakoids isolated from March (*Left*) and July 2018 (*Right*) samples are indicated. Most represented phosphosites identified are highlighted in red. LHCII proteins were separated by SDS-PAGE and stained with ProQ and Sypro. (*D*) Identified phosphosites in the N terminus, stromal loop, and C terminus of spruce PSBS proteins, PSBS_A and PSBS_B, of isolated thylakoids of sun needles from March 2018 (*Left*) and July 2018 (*Right*). Thylakoid proteins were separated by SDS-PAGE and stained with ProQ and Sypro. Phosphosites identified only in March 2018 are indicated in red and phosphosites identified in both March and July 2018 are indicated in blue. Gels in *C* and *D* were loaded on equal chlorophyll basis (4 μg).

main difference in their number of Ser and Thr residues in the N terminus (*SI Appendix*, Fig. S5*A*).

The new and highest molecular mass LHCII phosphoproteins massively present in sustained NPQ samples (Fig. 2 *A* and *B*) were identified to mainly contain the LHCB1_A isoform (Fig. 2*C* and Dataset S1). An N-terminal tryptic peptide of the LHCB1_A isoform was found with two or three different Thr and Ser residues simultaneously phosphorylated and was therefore assigned as triply phosphorylated LHCII (3p-LHCII) (*SI Appendix*, Figs. S6 and S7 and Dataset S1). These phosphorylations at the N terminus of LHCB1_A were likely causing the shift to higher apparent molecular mass during electrophoretic separation. The canonical LHCII bands 1 and 2 in spruce consisted mainly of both LHCB1_A and LHCB1_B isoforms with single phosphorylations on several Ser residues, while no triply phosphorylated N-terminal peptides were found. The canonical LHCII band 3 contained mainly LHCB2, which was singly phosphorylated. The phosphorylations of LHCB1_ A, LHCB1_B and LHCB2 in the three canonical LHCII bands could be identified in the sustained NPQ samples as well as in the summer samples (Dataset S1).

PSBS in spruce has two isoforms, PSBS_A and PSBS_B (*SI Appendix*, Fig. S5*B*). They both conserve the two protonatable Glu residues in the lumen-exposed regions, important for function of PSBS in qE (33). The largest sequence divergence between the isoforms was observed in the stromal loop. MS/MS analysis of PSBS from sustained NPQ samples (March 2018) identified several peptides with singly phosphorylated Thr or Ser residues in the stroma-exposed regions (N terminus, stromal loop, and C terminus) (Fig. 2*D*, red letters, and Dataset S1). Two Ser phosphosites were found phosphorylated also in the PSBS_A isoform in summer samples (Fig. 2*D*, blue letters, and Dataset S1). Although PSBS_A and PSBS_B share most of the phosphosites, fewer phosphopeptides were identified for PSBS_B.

Relaxation of Sustained NPQ and Dephosphorylation of 3p-LHCII and p-PSBS in Artificial Recovery Conditions. To find out whether the accumulation of 3p-LHCII and p-PSBS is linked to sustained NPQ, spruce branches of sun- and shade-exposed trees collected in March 2018 (sustained NPQ) and July 2018 (summer sample as a control) were subjected to an artificial recovery condition of Fv/Fm in darkness at +7 °C for 96 h. Darkness was selected on

purpose to follow only the recovery of sustained NPQ and preventing the recovery from photoinhibition, the process that requires light for several different subreactions of the PSII repair cycle (for a review, see ref. 8).

Fv/Fm was restored under recovery conditions from 0.38 to a maximum of 0.68 in shade-exposed needles and in sun-exposed needles from 0.10 to 0.53 (Fig. 3*A*). This maximal restoration of Fv/Fm, in relation to the level recorded for nonsustained NPQ needles of the previous month (February 2018; Fv/Fm 0.73), accounted for sustained NPQ experienced in March 2018 by the shade (41%) and sun (59%) needles, respectively. The rest of Fv/Fm decline, not restored in darkness, is assigned to PSII photoinhibition and accounted for 9% and 27% of Fv/Fm in shade and sun needles, respectively. In parallel, protein phosphorylation levels of isolated thylakoids were checked from 0-, 24-, and 96-h recovery time points via staining the gels with Sypro and ProQ (*SI Appendix*, Fig. S8) and by immunoblotting with p-Thr antibody (Fig. 3*B*). P-Thr antibody recognized in sustained NPQ samples both p-PSBS and a 3p-LHCII doublet that was similar to that observed with ProQ (Fig. 2*B*, indicated by red arrow, and *SI Appendix*, Fig. S8). Strong parallel decrease in Thr phosphorylations of p-PSBS and 3p-LHCII was evident during the first 24-h recovery of sustained NPQ needles. Dephosphorylation of p-D2 and p-LHCII also occurred while the dephosphorylation of the D1 protein could not be assessed due to comigration with p-LHCII bands in spruce. The dephosphorylation response in shade samples was similar (*SI Appendix*, Fig. S8 *B–D*). Control summer needles, with constant Fv/Fm all through the experiment, showed an increase in phosphorylation of canonical LHCII proteins under artificial recovery conditions (Fig. 3 *A* and *B*).

In line with restoration of Fv/Fm (Fig. 3*A*), the light curve experiments demonstrated an overall increase of Y(II) and Y(NPQ) during recovery from sustained NPQ (Fig. 3*C* and *SI Appendix*, Fig. S9), implying regain of photosynthetic and regulatory NPQ capacity. This was driven by a decrease of Y(NO) (*SI Appendix*, Fig. S9), as sustained NPQ (low Fv/Fm) manifests as high Y(NO). As PSII activity increased during recovery from sustained NPQ, a decrease of donor side limitation of PSI, Y(ND), was observed. This was accompanied by an increase of Y(I) in sun and shade needles (*SI Appendix*, Fig. S9). At low

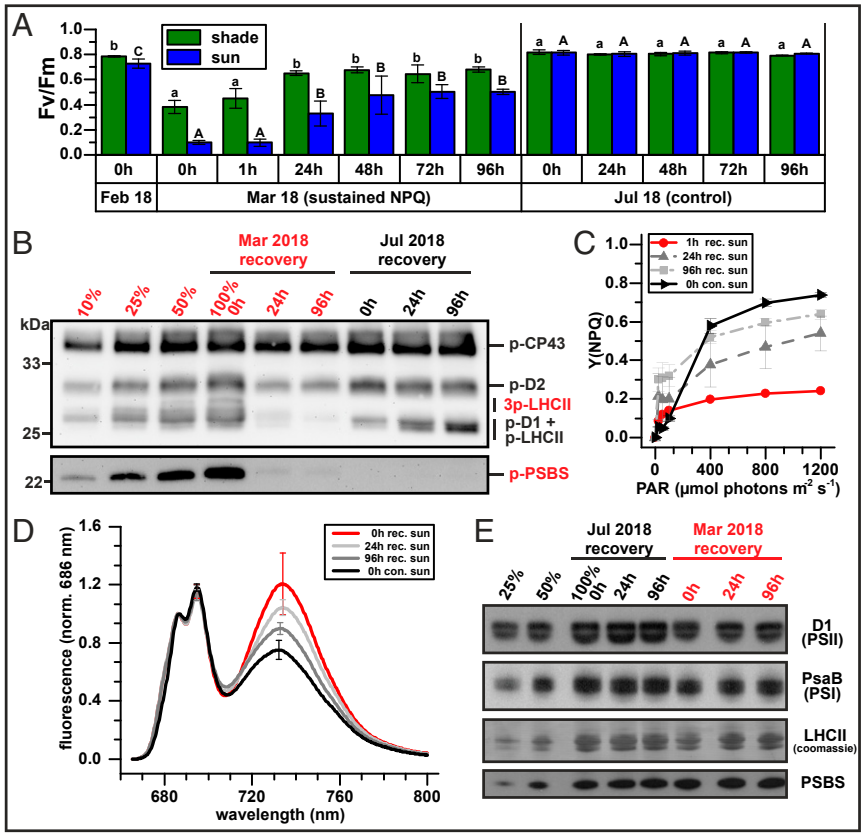

Fig. 3. Artificial recovery from sustained NPQ conditions. Recovery experiments were performed in darkness and 7 °C. (*A*) Recovery of maximum quantum yield of PSII photochemistry (Fv/Fm) with respect to February 2018 at different time points in shade (green bars) and sun (blue bars) needles from sustained NPQ in March 2018. July 2018 samples treated in the same way are shown as a control. Average of three biological replicates with SDs are shown. Letters (shade = lowercase, sun = uppercase) represent statistically significant groups, which were individually tested for each month and habitat (one-way ANOVA, Bonferroni, $P < 0.05$). (*B*) Antiphospho-threonine (p-Thr) immunoblot of thylakoid proteins isolated from sun needles after 0, 24, and 96 h of artificial recovery from sustained NPQ and from July 2018 needles as a control. P-Thr immunoblot of p-PSBS is shown with longer exposure time. The 0-h March 2018 sample was used as 100% protein loading control with dilutions of 50%, 25%, and 10%. Gel was loaded on equal chlorophyll basis (1 µg). (*C*) Quantum yield of regulatory nonphotochemical quenching, Y(NPQ), from light curve experiments of sun needles during artificial recovery. Average of three biological replicates with SDs are shown, except for 1-h samples from March 2018, for which only the least-quenched (highest Fv/Fm) replicate is shown (*SI Appendix*). (*D*) The 77 K fluorescence emission spectra from isolated thylakoids of sun needles during artificial recovery. Fluorescence spectra (excitation at 480 nm) were normalized to 686-nm peak. Average of three biological replicates with SDs are shown. (*E*) Immunoblots of thylakoid proteins isolated from sun needles after 0, 24, and 96 h of artificial recovery from sustained NPQ and control conditions. Thylakoid proteins were probed with D1/PsbA (PSII), PsaB (PSI), and PSBS antibody. LHCII proteins were visualized with Coomassie protein stain. The July 2018 sample was used as 100% loading control of proteins, with dilutions of 50% and 25%. Gel was loaded on equal chlorophyll basis (1 µg).

actinic light intensities, the recovery of Y(I) was counteracted by a small increase in acceptor side limitation, Y(NA). In comparison to sun needles, the recovery phenotype of shade needles was similar but smaller (*SI Appendix*, Fig. S9). Exposure of July 2018 sun and shade control needles to the same artificial recovery experiment revealed no pronounced changes in PSII and PSI parameters (*SI Appendix*, Fig. S10). The differences in Y(II) between needles recovered from sustained NPQ and the control summer needles likely reflected differences in acclimation states to winter and summer conditions.

To get insights into changes in energy distribution between the two photosystems, we next recorded the 77 K fluorescence emission spectra from thylakoids isolated in the course of the recovery experiment of both the sustained NPQ and the control summer needles. The 77 K fluorescence spectra showed two clear PSII peaks at 686 and 695 nm and one broad PSI peak around 734 nm (Fig. 3*D*), the latter shifting in some samples between 733 and 735 nm. Sustained NPQ samples had a higher PSI/PSII (F734/F686) fluorescence ratio compared to summer control samples, and the ratio decreased during recovery. This effect was more pronounced in sun compared to shade needles and absent from summer control samples (*SI Appendix*, Fig. S11). Moreover, the sustained NPQ samples showed a distinct shoulder at 680 nm, reflecting an increased amount of detached LHCII, which remained unchanged throughout the recovery.

It was finally checked whether the recovery from sustained NPQ was accompanied by changes in the amounts of the PSI, PSII, LHCII, and PSBS proteins (Fig. 3*E*). Using antibodies specific for PsbA/D1 (PSII) and PsaB (PSI), the immunoblotting analysis revealed that PSII and PSI were present in lower amounts in sustained NPQ samples compared to the summer control. Yet, the amounts of PSII and PSI did not change in darkness during the recovery experiment from sustained NPQ. Similarly, the amount of total LHCII (stained with Coomassie) remained unchanged, as well as that of the PSBS protein, indicating that changes in the level of phosphorylation were not connected to changes in protein amount.

Screening of 2016 to 2019 Needles for Accumulation of 3p-LHCII and p-PSBS in the Thylakoid Membrane. During the sampling period 2016 to 2019, only in March 2018 were the light and temperature conditions challenging enough to induce sustained NPQ in spruce thylakoids (Fig. 1 *A* and *B*). To evaluate whether the 3p-LHCII and p-PSBS are confined only to the conditions of sustained NPQ, their presence in spruce thylakoids was next investigated across the other winter, early spring, and summer samples by ProQ and Sypro staining, as well as by immunoblotting with p-Thr antibody of thylakoid proteins separated in 1D SDS-PAGE. Interestingly, we also found 3p-LHCII and p-PSBS in February 2017, January 2018, and January/February 2019 samples (Fig. 4 *A*–*D*), yet in lower amounts than in March 2018 samples of sustained NPQ. Similarly, in January 2016 3p-LHCII was recorded (*SI Appendix*, Fig. S12).

Immunoblotting with p-Thr antibody revealed that 3p-LHCII phosphorylation (Fig. 4*C*) coincided with the presence of p-PSBS (Fig. 4*D*) in the same winter months. Similar to artificial recovery experiments (Fig. 3), the amount of phosphorylated PSBS was not linked to protein amount of PSBS, as shown by the immunoblot with PSBS antibody (Fig. 4*E*).

To test whether the relatively high abundance of 3p-LHCII and p-PSBS in winter months, beside the March 2018 sustained NPQ sample, was accompanied by the presence of the CP43-less PSII subcomplex (Fig. 2 *A* and *B*), thylakoids were isolated from the corresponding samples, separated in 2D-lpBN/SDS-PAGE and their protein subunits stained with Sypro and ProQ (*SI Appendix*, Figs. S13–S15). Only traces of CP43-less PSII was visible in nonsustained NPQ winter samples, suggesting that photoinhibition of PSII is linked to sustained NPQ.

Closer inspection of the light and temperature conditions at different sampling times (Fig. 4*F*) revealed that p-PSBS and 3p-LHCII were present only when the average daily temperatures were ≤−4 °C. Dynamic regulation of the phosphorylation of both proteins is well highlighted in the sampling points of January, February, and March 2018. Here, 3p-LHCII and p-PSBS were both present at freezing temperatures in January and March

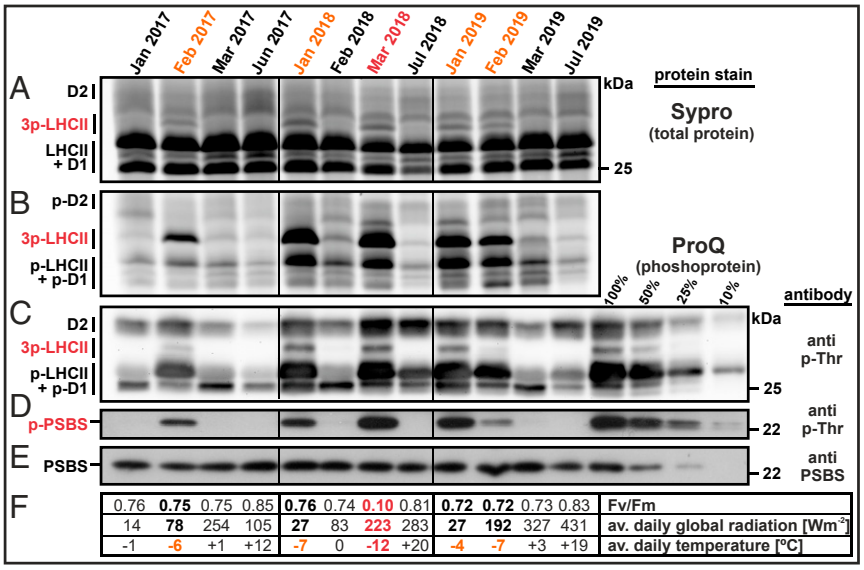

Fig. 4. Seasonal variation in accumulation of 3p-LHCII and p-PSBS in thylakoid membranes of spruce. (*A*–*E*) Comparison of 3p-LHCII and p-PSBS accumulation in January, February, March, and June/July thylakoid membranes isolated from samples collected in 2017 to 2019 and subjected to SDS-PAGE. (*A*–*C*) LHCII molecular mass region stained with (*A*) Sypro, (*B*) ProQ, and immunoblotted with (*C*) phospho-threonine (p-Thr) antibody. p-D1 migrates in the same region but overlaps with p-LHCII and therefore is not indicated. Gel was loaded on equal chlorophyll basis (4 μg). (*D* and *E*) PSBS molecular mass region of immunoblots probed with (*D*) p-Thr antibody and (*E*) PSBS antibody. Gel was loaded on equal chlorophyll basis (1 μg). The March 2018 sample was used as 100% loading control, with dilutions of 50%, 25%, and 10%. (*F*) Maximum quantum yield of PSII photochemistry (Fv/Fm), average daily global radiation (W m^{-2}) and temperature (°C) of the sampling day.

2018, but absent from February 2018, when the temperature was higher (Dataset S2). Importantly, sustained NPQ occurred only when both the freezing temperatures and average daily irradiance levels above 200 Wm^{-2} (global radiation) had prevailed for several days, like in March 2018 (Dataset S2).

Artificial Induction of Sustained NPQ and Accumulation of 3p-LHCII and p-PSBS. Spruce experiments from natural environments revealed that the accumulation of 3p-LHCII and p-PSBS in the thylakoid membrane is profoundly influenced by the duration and severity of freezing temperatures coinciding with high daily irradiance levels (Fig. 4 and Dataset S2). This prompted us to perform a more controlled artificial winter experiment by using spruce branches from their natural habitats, at winter acclimated but nonsustained NPQ state, and transferring them to −20 °C with daily illumination gradually reaching the maximum photon flux density of 900 μmol photons m^{-2} s^{-1} (*SI Appendix*, Fig. S16). In total, four day/night cycles were applied, whereas the other set of spruce branches was kept in darkness at −20 °C.

As demonstrated in Fig. 5, our artificial freezing treatment induced limited decline in Fv/Fm, but importantly, it specifically occurred only in illuminated needles and reached the lowest value in 96 h with Fv/Fm ± SD being 0.43 ± 0.01 as compared to 0.68 ± 0.04 in the beginning of the experiment. In parallel, a small amount of p-PSBS accumulated in the thylakoid membrane, again only in illuminated needles (Fig. 5). To estimate the fraction of observed decline in Fv/Fm that was due to sustained NPQ or to PSII photoinhibition, the rest of the needles light-treated at −20 °C were transferred to recovery conditions at +7 °C in darkness for 96 h. Restoration of Fv/Fm in these needles was limited (Fv/Fm 0.48 ± 0.02 after 96 h), implying the induction of only marginal sustained NPQ (~7%), with much higher proportion of the decline in Fv/Fm being caused by PSII photoinhibition during the given artificial experiment. Appearance of only minor accumulation of p-PSBS in these needles, as compared to that of the March 2018 shade and sun samples of much stronger sustained NPQ (Fig. 2*B*), is in line with a close relationship between the appearance and strength of sustained NPQ and the accumulation p-PSBS (Fig. 5).

Accumulation of 3p-LHCII in the artificial freezing temperature experiment was only partial, particularly evident by anti–p-Thr blotting, as compared to March 2018 samples (Fig. 5). Importantly, however, 3p-LHCII was rapidly induced both in light and in darkness, already during the first 24 h, and remained at the same level for 96 h.

Discussion

Overwintering of evergreen conifers relies on a wide range of different strategies (1), which are employed more or less intensively depending on the severity of the winter conditions, particularly in terms of the temperatures and daily light conditions. As to the protection of the photosynthetic apparatus, the sustained NPQ represents the most efficient hardening mechanism. It protects the photosynthetic apparatus by harmless thermal dissipation of excitation energy, in particular under freezing temperatures when CO_2 fixation is blocked but light is still absorbed by photosynthetic pigments, the condition that in the absence of sustained NPQ would favor massive production of reactive oxygen species. However, development of winter acclimation, with sustained NPQ as the most stringent acclimation

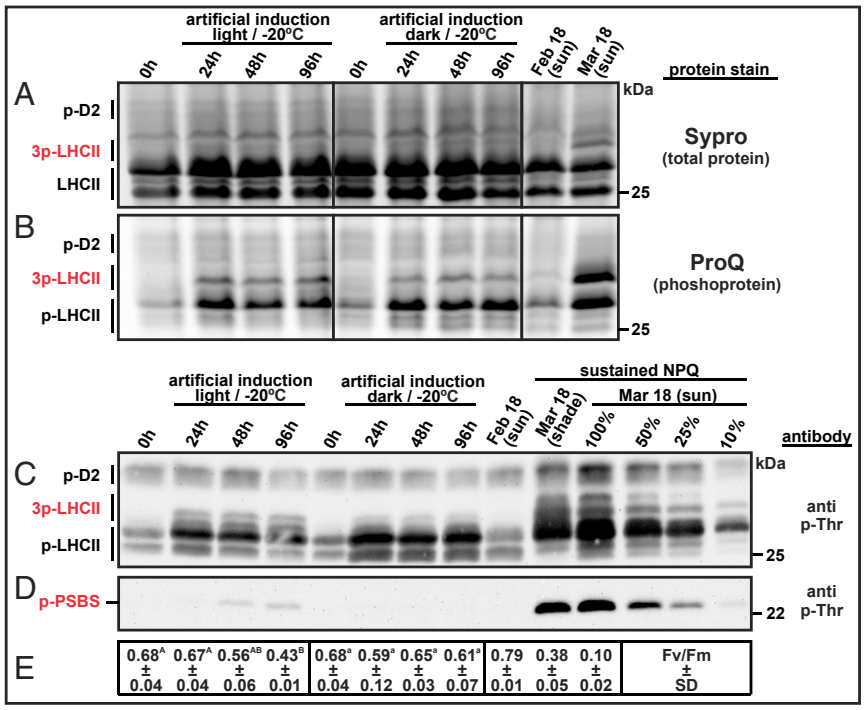

Fig. 5. Artificial induction of 3p-LHCII and p-PSBS upon freezing temperature and development of sustained NPQ. (*A*–*D*) Comparison of 3p-LHCII and p-PSBS accumulation in thylakoid membranes isolated from sun-exposed needles (outside temperature 7 °C; 0 h) and subsequently subjected to freezing temperature (−20 °C) for 4 d either in the presence of 900-μmol photons m^{-2} s^{-1} or in complete darkness. (*A*–*C*) Molecular mass region corresponding to p-D2, 3p-LHCII, and p-LHCII stained with (*A*) Sypro, (*B*) ProQ, and immunoblotted with (*C* and *D*) phospho-threonine (p-Thr) antibody. The February 2018 and March 2018 sun samples were included as comparison in *A* and *B*. In *C* and *D*, the February 2018 sun, March 2018 shade and March 2018 sun were added for comparison, and the March 2018 sun was used as 100% loading control, with dilutions to 50%, 25%, and 10%. Gels were loaded on equal chlorophyll basis (4 μg in *A* and *B*, 1 μg in *C* and *D*). (*D*) PSBS molecular mass region of immunoblots probed with p-Thr antibody. (*E*) Maximum quantum yield of PSII photochemistry (Fv/Fm) at the sampling points. Letters (dark = lowercase, light = uppercase) represent significantly different groups, which were individually tested for each condition (ANOVA on ranks, Kruskal–Wallis, $P < 0.05$).

state, occurs gradually upon shortening of the day length in autumn and decreasing of the temperature together with still prevailing moderate to high light intensities (1, 34). Sustained NPQ is apparently built up on the top of the development of other winter acclimation processes on the chloroplast level, including accumulation of zeaxanthin (11, 12), changes in lipid composition of the thylakoid membrane (1), or reorganization of thylakoids with disappearance of the appressed membranes (16–18). These acclimation strategies apparently also decline the photochemical efficiency of PSII (Fv/Fm), but to a much minor extent than the development of sustained NPQ (Figs. 1, 3, and 4). Yet, the specific molecular switches involved in induction and relaxation of sustained NPQ have remained elusive.

Thylakoid Protein Phosphorylations Related to Sustained NPQ. To understand the mechanisms for switching sustained NPQ on and off, we investigated spruce needles collected from natural environments in southern Finland from 2016 to 2019. Temperatures below 0 °C occurred for only a few weeks per year and temperatures below −10 °C were recorded only for a few consecutive days (Fig. 1*A* and Dataset S2), and when coinciding with high light intensities (particularly March 2018), sustained NPQ was observed in spruce needles of both the sun- and shade-exposed trees (Fig. 1 *A* and *B*). During milder winter months, the nonsustained NPQ needles remained functional, although with reduced PSII and PSI capacity (Fig. 1*C* and *SI Appendix*, Figs. S1 and S2). This is in agreement with previous studies of various evergreen species (35–39) and highlights an opportunistic winter acclimation process (40) by ensuring flexible response to environmental changes (38). Comparison of spruce Y(NPQ) between sustained NPQ and nonsustained NPQ winter and summer samples (Fig. 1*D* and *SI Appendix*, Fig. S1) revealed that only upon the induction of sustained NPQ (March 2018 samples) did the capacity for maximal regulatory NPQ decline, but was not completely eliminated. Conversely, the other winter and all summer samples demonstrated a high and unchanged capacity for regulatory NPQ. This strongly suggests that the development of sustained NPQ is built on top of already existing regulatory NPQ components, and is supported by the regain of regulatory NPQ capacity during recovery from sustained NPQ (Fig. 3*D*).

In a search for missing regulatory components of sustained NPQ, we addressed a potential role of thylakoid protein complexes and their posttranslational phosphorylations, which are known to mediate various acclimation strategies of the photosynthetic apparatus to changing environmental cues (21, 24, 41). Initial comparison of sustained NPQ needles with control summer samples revealed two specific and previously uncharacterized phosphorylations of thylakoid proteins in sustained NPQ needles (Fig. 2 *A* and *B*). First, the LHCB1_A isoform was found to be triply phosphorylated at its N terminus (3p-LHCII) (Fig. 2*C*, and Dataset S1) and second, the PSBS protein was found phosphorylated at multiple stromal exposed sites (p-PSBS) (Fig. 2*D* and Dataset S1). The desphosphorylation of 3p-LHCII and p-PSBS during artificial recovery from sustained NPQ (Fig. 3 *A* and *B*) strongly suggests that both are linked to the sustained NPQ mechanism. However, these phosphorylations recorded in the field experiments were not limited to sustained NPQ conditions, but were found also in nonsustained NPQ thylakoids of winter samples collected during freezing temperatures ≤−4 °C (Fig. 4, *SI Appendix*, Fig. S12, and Dataset S1).

To better delineate the occurrence of 3p-LHCII and p-PSBS in spruce thylakoid membrane and their relation to sustained NPQ, spruce branches were collected from their natural habitat during early spring in a nonsustained NPQ state and subjected to artificial freezing (−20 °C) in light and in darkness (Fig. 5). Although only a limited amount of sustained quenching was obtained (7%), the appearance of p-PSBS in the thylakoid membrane coincided with development of sustained NPQ, both occurring only in light, and developed gradually within 2 to 4 d. The 3p-LHCII accumulation was different and concerned only part of 3p-LHCIIs in comparison to spruce collected from natural conditions during freezing temperatures. Additionally, the accumulation of 3p-LHCII was fully accomplished already during the first day and occurred independently of light (Fig. 5), providing evidence that 3p-LHCII is not directly involved in sustained NPQ but rather operates as a prerequisite for development of sustained NPQ. The experiments on artificial induction of sustained NPQ also clearly demonstrated that there is a strict control, based both on physiological and environmental conditions, that eventually determines the shares of sustained NPQ and photoinhibition, which together reduce Fv/Fm parameter under bright winter days.

Putative Role of 3p-LHCII in Development of Sustained NPQ. Of the LHCII proteins in spruce, only the LHCB1_A isoform was found triply phosphorylated (Fig. 2*C*). This is likely due to the fact that the LHCB1_A and LHCB1_B isoforms in spruce [and pine (32)] have different N-terminal sequences with varying numbers of Ser and Thr residues (Fig. 2*C*). The N terminus of LHCB1 in land plants is, in general, less conserved in length and sequence composition than LHCB2 (*SI Appendix*, Fig. S5*A*). LHCB2 N-terminal phosphorylation is specifically responsible for formation of the state-transition complex (PSI–LHCI–LHCII) (42–44) in various plant species and it is highly unlikely that LHCB1_A triple phosphorylation in spruce would be involved in this mechanism. Instead, we consider the triple phosphorylation of LHCB1_A (3p-LHCII) specific for thylakoid reorganization in conifers during winter (1, 10).

In analogy to the function of the singly phosphorylated p-LHCB1 isoform in loosening the thylakoid stacking in angiosperm chloroplasts (25, 41, 45), a similar but more stringent role is hypothesized for 3p-LHCII in spruce. The presence of 3p-LHCII coincides with freezing temperatures (Figs. 4 *A*, *C*, and *E* and 5), suggesting that 3p-LHCII is responsible for destacking of the appressed grana thylakoids during winter acclimation of evergreen members of Pinaceae (16–18). The increase in negative charges in the partition gap between the appressed thylakoid membranes by 3p-LHCII most likely results in a higher repulsion and ultimately leads to full separation of the appressed membranes (Fig. 6). The destacking and linearization of thylakoids upon formation of 3p-LHCII could, in turn, lead to loosening of the lateral heterogeneity of photosystems and thereby increase the chance for PSII–PSI spillover, which has been suggested to be involved in sustained NPQ (1, 17, 46). Conversely, a coherent restoration of Fv/Fm and dephosphorylation of 3p-LHCII occurred upon recovery of spruce needles from sustained NPQ (Fig. 3 *A* and *B*). Moreover, the reestablishment of summer-like excitation energy distribution between the two photosystems, deduced from the 77 K chlorophyll fluorescence spectra (Fig. 3*D*), is in line with a reduction in the putative PSI-spillover quenching. It is thus conceivable that relaxation of sustained NPQ, together with 3p-LHCII dephosphorylation, gradually lead to thylakoid restacking and lateral segregation of the two photosystems. In fact, reversible 3p-LHCII phosphorylation seems to be a frequent event and apparently involved in an intermediate state when freezing and nonfreezing temperatures vary during winter (Fig. 4), and likely provides a relatively rapid means for contribution to the development of sustained NPQ, upon critical lowering of the temperature.

Putative Role of p-PSBS in Development of Sustained NPQ. Two PSBS isoforms were identified in spruce, PSBS_A and PSBS_B, both with phosphorylations on several Ser and Thr residues at the stromal exposed regions of the protein (Fig. 2*D*). Of the phosphosites identified, two Ser residues were found phosphorylated also in summer conditions (Fig. 2*D*, blue letters), hence these are not involved in winter acclimation. PSBS has not been previously described as a phosphoprotein in the photosynthesis literature, yet two PSBS phosphopeptides have been identified by means of

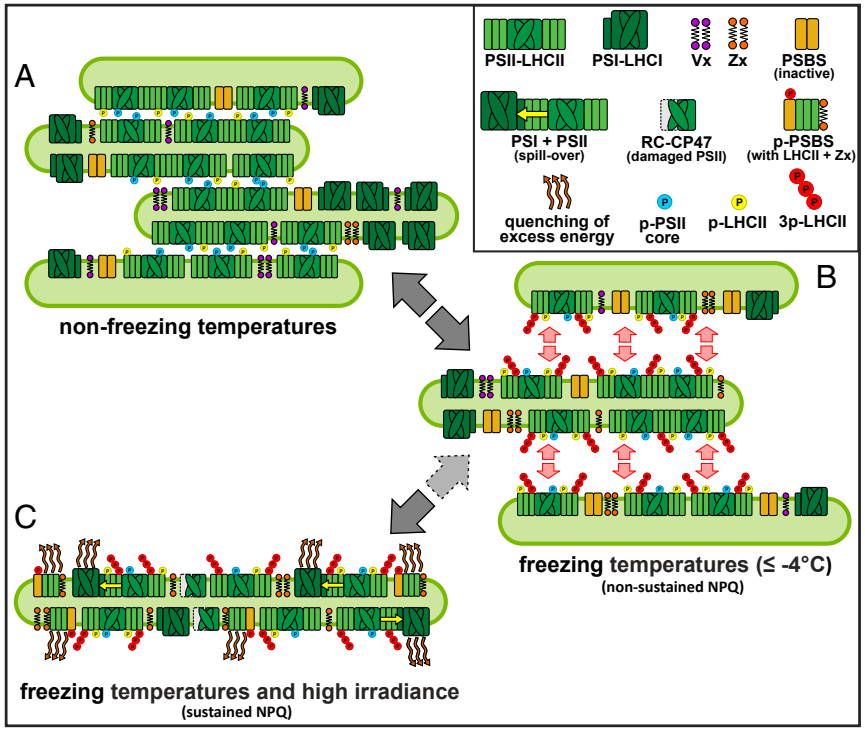

Fig. 6. Proposed model for thylakoid winter acclimation and induction of sustained NPQ in spruce. (*A*) In nonfreezing temperatures spruce thylakoid architecture is well separated in grana stacks and interconnecting stroma lamellae. PSII–LHCII supercomplexes are mostly found in appressed grana membranes, while PSI–LHCI complexes are confined to stroma lamellae (lateral heterogeneity). Only canonical PSII core and singular LHCII phosphorylations can occur depending on the light intensity. The LHCII antenna is functionally mostly connected to PSII and the photosynthetic apparatus is capable of regulatory NPQ. PSBS can be activated by light but otherwise is present in its inactive form (dimer) and violaxanthin (Vx) is the dominant xanthophyll. (*B*) Upon freezing temperatures, an intermediate, yet not sustained NPQ state is reached. The regulatory NPQ can still function with full capacity and possibly includes the accumulation of zeaxanthin (Zx). This state is characterized by accumulation of 3p-LHCII, repulsing the tightly packed grana thylakoids and eventually leading to destacking of appressed membranes. This easily revertible state is strongly dependent on temperature and also functions as a transition to sustained NPQ when appropriate. (*C*) Upon prolonged freezing temperatures and concomitant exposure to high light, the sustained NPQ state is engaged. This occurs in concert with partial PSII photoinhibition, which is speculated to function as a trigger for induction of sustained NPQ. Thus, the photodamaged PSII would—cooperatively with 3p-LHCII, p-PSBS, and Zx—induce a sustained aggregation of LHCII to allow efficient quenching of excitation energy as heat. At this stage the phosphorylation of PSBS would prevent its inactivation making sustained NPQ independent of lumen acidification. Photosynthetic complexes: PSII–LHCII (light green), PSI–LHCI (dark green), PSBS (orange). Xanthophyll pigments: violaxanthin (Vx, purple) and zeaxanthin (Zx, dark orange). Different protein phosphorylations: PSII core phosphorylation (p-PSII core, blue), canonical LHCII phosphorylation (p-LHCII, yellow), and triple phosphorylated LHCB1_A (3p-LHCII, red).

phospho-enrichment in *Arabidopsis* (47). Although, we identified fewer peptides for the PSBS_B isoform than for the A isoform, both isoforms could have important functions during winter acclimation. It is noteworthy, that both PSBS isoforms are highly similar but show sequence divergence in the stromal loop between the transmembrane helices TM2 and TM3 (*SI Appendix*, Fig. S5*B*).

The PSBS protein is an essential component of regulatory NPQ, in particular qE, and serves as a pH sensor via two Glu residues at lumen exposed loops (33, 48). Upon acidification of the lumen, dimeric PSBS monomerizes (49–51) and induces a quenching state in the LHCII antenna. Other interaction partners of PSBS have also been suggested (50, 51), although LHCII likely is a prominent partner (49). In spruce, the protonatable Glu residues of PSBS are conserved (*SI Appendix*, Fig. S5*B*), which makes it highly likely that spruce PSBS function in qE is conserved. Our data on the extent of PSBS phosphorylation coinciding with the development and the strength of sustained NPQ (Fig. 5) and a rapid p-PSBS dephosphorylation upon relaxation of sustained NPQ in favorable conditions (Fig. 3 *A* and *B*) suggest a crucial role for p-PSBS in sustained NPQ.

For the functional role of p-PSBS during sustained NPQ, it can be hypothesized that phosphorylation of specific residues would induce a conformational change in PSBS (Fig. 2*D*). This possibly promotes the stabilization of active PSBS and affects its interaction with other partners, allowing long-term sustained quenching for example via LHCII. Previous studies on conifer species have shown that zeaxanthin accumulation correlates well with formation of a sustained NPQ state (11–13). Additionally, aggregation of LHCII has been previously suggested to play a role during sustained NPQ (1), like in regulatory NPQ (52, 53). Increased amounts of disconnected LHCII antenna (Fig. 3*D*) may indicate that LHCII aggregation is also present in the sustained NPQ of spruce. PSBS and zeaxanthin have been proposed to act as a seeding center (51) in enhancing the qE-dependent regulatory NPQ via LHCII aggregation (15, 54, 55). In this context, and incorporated into our model (Fig. 6), the role of p-PSBS could be to help keeping PSBS-Zea-LHCII aggregates locked in a quenching state to allow sustained NPQ in spruce. Most importantly, lumen acidification would not be required to maintain such locked-in quenched complex, which is an essential prerequisite to keep the sustained NPQ state in darkness.

Whichever the exact role of the phosphorylation in changing the conformation of PSBS, we hypothesize that the PSBS-dependent part of regulatory NPQ can be converted, under the right environmental conditions of freezing temperature and sufficiently high light intensity, into sustained NPQ, as has been suggested previously based on in vivo fluorescence studies (56). This would also explain the retention of high regulatory NPQ capacity observed throughout the winters and its decline only during sustained NPQ conditions (Fig. 1*D* and *SI Appendix*, Fig. S1).

Involvement of PSII Photoinhibition in Induction of Sustained NPQ. The artificially induced relaxation of sustained NPQ at 7 °C in darkness provided us with the means to investigate the involvement of PSII photoinhibition in sustained NPQ. This is because the repair of damaged PSII is light-dependent with respect to many subprocesses of the repair cycle (7, 57), including the PsbA (D1) translation initiation as well as many PSII assembly steps and the eventual photo activation (for a review, see ref. 8). During artificial recovery in darkness, the sun and shade needles restored Fv/Fm to a steady-state level within 24 h, respectively, however, not reaching the higher values of nonquenched winter needles (Fig. 3*A*). This difference in Fv/Fm value mostly represents PSII photoinhibitory quenching component (qI) and is well in line with the accumulation of the CP43-less (RC-CP47) PSII repair intermediate complex only in sustained NPQ needles (Fig. 2 *A* and *B*), in comparison to nonsustained NPQ samples (*SI Appendix*, Figs. S13–S15).

At first glance, the presence of PSII photoinhibition upon sustained NPQ seems to contradict the photoprotective function assigned to sustained NPQ. However, it could be argued that PSII photoinhibition is an unavoidable side product of extreme environmental conditions required to induce sustained NPQ, and such a transition would impair the capacity of PSII repair to keep pace with the damage to PSII. On the other hand, the accumulation of RC47-PSII might have an active role in induction of sustained NPQ. It is conceivable that photodamaged PSII, in concert with p-PSBS, jointly trigger the sustained NPQ state. This would occur only when photodamage to PSII exceeds the repair capacity and the regulatory NPQ capacity, present in spruce all through the winter (except for the strongest sustained NPQ state), gets overwhelmed (Fig. 6).

Concluding Remarks

Two previously unknown reversible phosphorylations in spruce thylakoid proteins, the triple phosphorylation of the N terminus of LHCB1_A isoform and the several phosphorylations of the PSBS protein, are hypothesized here as prerequisites for development of sustained NPQ (Fig. 6) in spruce. Importantly, these phosphorylation events are strictly under environmental regulation and require below-freezing daily temperatures for any significant accumulation of 3p-LHCB1_A and p-PSBS. In particular, the accumulation and dephosphorylation p-PSBS coincided, respectively, with the development and relaxation of the sustained NPQ state, and is thus suggested to allow development of sustained NPQ in evergreen needles on the demand of environmental cues. It seems that the same PSBS protein serves the regulatory NPQ and sustained NPQ in nonphosphorylated form and phosphorylated form, respectively. As to the mechanistic consequences of accumulation of 3p-LHCII in freezing temperatures and independently of light, we suggest it to play an essential role for promoting the destacking of the grana thylakoids typical for spruce upon winter acclimation, and thereby facilitates the PSI-spillover quenching (Fig. 6). In mechanistic terms, p-PSBS could keep the protein constitutively active under freezing temperatures in order to maintain sustained NPQ without a need for acidification of thylakoid lumen. Thus, on one hand, the phosphorylation events (3p-LHCII and p-PSBS) likely function as prerequisites for enabling the capacity to develop sustained NPQ but do not, as such, induce sustained NPQ. On the other hand, part of sustained NPQ is comprised by PSII photoinhibition, suggesting that photodamaged PSII provides the means for prompt triggering of sustained NPQ. It is plausible that the phosphorylation events together with PSII photodamage jointly induce relevant conformational changes in proteins and pigments to allow the conversion of regulatory NPQ to sustained NPQ, and vice versa.

Materials and Methods

Plant Material. Needles for all experiments were collected from *Picea abies* (Norway spruce) trees grown in a forest close to Turku, Finland (60°27′N, 22°16′E). Five trees were selected from sun- and shade-exposed habitats, respectively. South-facing branches (up to 2 m in height) were harvested around noon monthly during 2016 and from 2017 to 2019 during January, February, March, and June/July, placed in a light-tight plastic bag, and transported to the laboratory (~30 min). Sampling dates are indicated in Dataset S2. At freezing temperatures, branches were transported on ice. Upon arrival in the laboratory, needles were cut from branches and immediately used for parallel thylakoid isolations and in vivo fluorescence and absorption measurements. For artificial recovery and artificial induction experiments, see *SI Appendix*.

Thylakoid Isolation and Chlorophyll Determination. Mature needles from all five branches, separately collected from both the sun and shade habitats, were pooled and thylakoid isolations performed in dim light and on ice following the protocol from Grebe et al. (29). All buffers contained 10 mM NaF as phosphatase inhibitor to preserve thylakoid protein phosphorylations and the in vivo state of the thylakoid supercomplexes. Chlorophyll concentration was determined in 80% buffered acetone according to Porra et al. (58).

In Vivo Chlorophyll Fluorescence and P700 Difference Absorption. Mature needles of three of the five collected branches were randomly selected from sun and shade habitats, respectively. Simultaneous in vivo chlorophyll fluorescence and P700 difference absorption light curve experiments were performed with a Dual-PAM 100 (Heinz Walz). The details of the light curve experiments are reported in *SI Appendix*.

Gel Electrophoresis and MS Analysis. Spruce thylakoids were loaded on equal chlorophyll bases in the wells of both monodimensional 12% acrylamide (w/v) 6 M urea SDS-PAGE and in lpBN/PAGE. ProQ Diamond phosphoprotein and SYPRO Ruby total protein staining of 2D lpBN/SDS-PAGE gels were performed according to manufacturer's instructions (Invitrogen/Molecular Probes). Protein spots were excised from the gel and subjected to in-gel tryptic digestion as in Trotta et al. (25). The details of protein isolation, staining, and immunoblotting, as well as MS identification are described in *SI Appendix*. The MS proteomics data have been deposited to the ProteomeXchange Consortium via the PRIDE (59) partner repository with the dataset identifier PXD018941 and 10.6019/PXD018941.

ACKNOWLEDGMENTS. We thank Virpi Paakkarinen for her excellent technical assistance; and Tapio Ronkainen for invaluable help in construction of an "ad hoc" growth chamber, allowing programmed illumination of spruce needles at −20 °C, despite the Coronavirus disease 2019 pandemic and very limited access to the laboratories at the University of Turku. Mass spectrometers at the Turku Proteomics Facility, supported by Biocenter Finland, were used for phosphoprotein analyses. This research was funded by the European Union's Horizon 2020 research and innovation program (Grant Agreement 675006), the Academy of Finland Centers of Excellence project (307335), and the Jane and Aatos Erkko Foundation.

1. G. Öquist, N. P. A. Huner, Photosynthesis of overwintering evergreen plants. *Annu. Rev. Plant Biol.* **54**, 329–355 (2003).
2. C. Crosatti, F. Rizza, F. W. Badeck, E. Mazzucotelli, L. Cattivelli, Harden the chloroplast to protect the plant. *Physiol. Plant.* **147**, 55–63 (2013).
3. P. Horton, Optimization of light harvesting and photoprotection: Molecular mechanisms and physiological consequences. *Philos. Trans. R. Soc. Lond. B Biol. Sci.* **367**, 3455–3465 (2012).
4. A. V. Ruban, Nonphotochemical chlorophyll fluorescence quenching: Mechanism and effectiveness in protecting plants from photodamage. *Plant Physiol.* **170**, 1903–1916 (2016).
5. A. Malnoë, Photoinhibition or photoprotection of photosynthesis? Update on the (newly termed) sustained quenching component qH. *Environ. Exp. Bot.* **154**, 123–133 (2018).
6. P. Jahns, A. R. Holzwarth, The role of the xanthophyll cycle and of lutein in photoprotection of photosystem II. *Biochim. Biophys. Acta* **1817**, 182–193 (2012).
7. E. M. Aro, I. Virgin, B. Andersson, Photoinhibition of photosystem II. Inactivation, protein damage and turnover. *Biochim. Biophys. Acta* **1143**, 113–134 (1993).
8. S. Järvi, M. Suorsa, E.-M. Aro, Photosystem II repair in plant chloroplasts—Regulation, assisting proteins and shared components with photosystem II biogenesis. *Biochim. Biophys. Acta* **1847**, 900–909 (2015).
9. C. L. Amstutz *et al.*, An atypical short-chain dehydrogenase-reductase functions in the relaxation of photoprotective qH in Arabidopsis. *Nat. Plants* **6**, 154–166 (2020).
10. A. Verhoeven, Sustained energy dissipation in winter evergreens. *New Phytol.* **201**, 57–65 (2014).

11. C. Ottander, D. Campbell, G. Öquist, Seasonal changes in photosystem-II Organization and pigment composition in Pinus sylvestris. *Planta* **197**, 176–183 (1995).
12. A. S. Verhoeven, W. W. Adams, B. Demmig-Adams, Two forms of sustained xanthophyll cycle-dependent energy dissipation in overwintering Euonymus kiautschovicus. *Plant Cell Environ.* **21**, 893–903 (1998).
13. A. S. Verhoeven, A. Swanberg, M. Thao, J. Whiteman, Seasonal changes in leaf antioxidant systems and xanthophyll cycle characteristics in Taxus x media growing in sun and shade environments. *Physiol. Plant.* **123**, 428–434 (2005).
14. M. P. Johnson *et al*., Elevated zeaxanthin bound to oligomeric LHCII enhances the resistance of Arabidopsis to photooxidative stress by a lipid-protective, antioxidant mechanism. *J. Biol. Chem.* **282**, 22605–22618 (2007).
15. E. Kress, P. Jahns, The dynamics of energy dissipation and xanthophyll conversion in arabidopsis indicate an indirect photoprotective role of zeaxanthin in slowly inducible and relaxing components of non-photochemical quenching of excitation energy. *Front. Plant Sci.* **8**, 2094 (2017).
16. B. Martin, G. Öquist, Seasonal and experimentally induced changes in the ultrastructure of chloroplasts of Pinus silvestris. *Physiol. Plant.* **46**, 42–49 (1979).
17. B. Demmig-Adams, O. Muller, J. J. Stewart, C. M. Cohu, W. W. Adams, 3rd, Chloroplast thylakoid structure in evergreen leaves employing strong thermal energy dissipation. *J. Photochem. Photobiol. B* **152**, 357–366 (2015).
18. Q. Yang *et al*., Two dominant boreal conifers use contrasting mechanisms to reactivate photosynthesis in the spring. *Nat. Commun.* **11**, 128 (2020).
19. H.-W. Trissl, C. Wilhelm, Why do thylakoid membranes from higher plants form grana stacks? *Trends Biochem. Sci.* **18**, 415–419 (1993).
20. J. M. Anderson, Lateral heterogeneity of plant thylakoid protein complexes: Early reminiscences. *Philos. Trans. R. Soc. Lond. B Biol. Sci.* **367**, 3384–3388 (2012).
21. J.-D. Rochaix *et al*., Protein kinases and phosphatases involved in the acclimation of the photosynthetic apparatus to a changing light environment. *Philos. Trans. R. Soc. Lond. B Biol. Sci.* **367**, 3466–3474 (2012).
22. P. Pesaresi, M. Pribil, T. Wunder, D. Leister, Dynamics of reversible protein phosphorylation in thylakoids of flowering plants: The roles of STN7, STN8 and TAP38. *Biochim. Biophys. Acta* **1807**, 887–896 (2011).
23. W. S. Chow, E.-H. H. Kim, P. Horton, J. M. Anderson, Granal stacking of thylakoid membranes in higher plant chloroplasts: The physicochemical forces at work and the functional consequences that ensue. *Photochem. Photobiol. Sci.* **4**, 1081–1090 (2005).
24. M. Tikkanen, E.-M. Aro, Integrative regulatory network of plant thylakoid energy transduction. *Trends Plant Sci.* **19**, 10–17 (2014).
25. A. Trotta *et al*., The role of phosphorylation dynamics of CURVATURE THYLAKOID 1B in plant thylakoid membranes. *Plant Physiol.* **181**, 1615–1631 (2019).
26. M. Suorsa *et al*., Light acclimation involves dynamic re-organization of the pigment-protein megacomplexes in non-appressed thylakoid domains. *Plant J.* **84**, 360–373 (2015).
27. M. Grieco, M. Suorsa, A. Jajoo, M. Tikkanen, E.-M. Aro, Light-harvesting II antenna trimers connect energetically the entire photosynthetic machinery—Including both photosystems II and I. *Biochim. Biophys. Acta* **1847**, 607–619 (2015).
28. M. Yokono, A. Takabayashi, S. Akimoto, A. Tanaka, A megacomplex composed of both photosystem reaction centres in higher plants. *Nat. Commun.* **6**, 6675 (2015).
29. S. Grebe *et al*., The unique photosynthetic apparatus of Pinaceae: Analysis of photosynthetic complexes in Picea abies. *J. Exp. Bot.* **70**, 3211–3225 (2019).
30. R. Kouřil, L. Nosek, J. Bartoš, E. J. Boekema, P. Ilík, Evolutionary loss of light-harvesting proteins Lhcb6 and Lhcb3 in major land plant groups—Break-up of current dogma. *New Phytol.* **210**, 808–814 (2016).
31. M. Grieco, A. Jain, I. Ebersberger, M. Teige, An evolutionary view on thylakoid protein phosphorylation uncovers novel phosphorylation hotspots with potential functional implications. *J. Exp. Bot.* **67**, 3883–3896 (2016).
32. S. Jansson, P. Gustafsson, Type I and type II genes for the chlorophyll a/b-binding protein in the gymnosperm Pinus sylvestris (Scots pine): cDNA cloning and sequence analysis. *Plant Mol. Biol.* **14**, 287–296 (1990).
33. X. P. Li *et al*., Regulation of photosynthetic light harvesting involves intrathylakoid lumen pH sensing by the PsbS protein. *J. Biol. Chem.* **279**, 22866–22874 (2004).
34. L. V. Savitch *et al*., Two different strategies for light utilization in photosynthesis in relation to growth and cold acclimation. *Plant Cell Environ.* **25**, 761–771 (2002).
35. A. G. Ivanov *et al*., Photosynthetic electron transport adjustments in overwintering Scots pine (Pinus sylvestris L.). *Planta* **213**, 575–585 (2001).
36. H. G. Weger, S. N. Silim, R. D. Guy, Photosynthetic acclimation to low temperature by Western red cedar seedlings. *Plant Cell Environ.* **16**, 711–717 (1993).
37. J. B. Nippert, R. A. Duursma, J. D. Marshall, Seasonal variation in photosynthetic capacity of montane conifers. *Funct. Ecol.* **18**, 876–886 (2004).
38. P. Kolari *et al*., Field and controlled environment measurements show strong seasonal acclimation in photosynthesis and respiration potential in boreal Scots pine. *Front. Plant Sci.* **5**, 717 (2014).
39. J. D. Marshall, G. E. Rehfeldt, R. A. Monserud, Family differences in height growth and photosynthetic traits in three conifers. *Tree Physiol.* **21**, 727–734 (2001).
40. I. Ensminger *et al*., Intermittent low temperatures constrain spring recovery of photosynthesis in boreal Scots pine forests. *Glob. Change Biol.* **10**, 995–1008 (2004).
41. R. Fristedt *et al*., Phosphorylation of photosystem II controls functional macroscopic folding of photosynthetic membranes in Arabidopsis. *Plant Cell* **21**, 3950–3964 (2009).
42. M. Pietrzykowska *et al*., The light-harvesting chlorophyll a/b binding proteins Lhcb1 and Lhcb2 play complementary roles during state transitions in Arabidopsis. *Plant Cell* **26**, 3646–3660 (2014).
43. A. Crepin, S. Caffarri, The specific localizations of phosphorylated Lhcb1 and Lhcb2 isoforms reveal the role of Lhcb2 in the formation of the PSI-LHCII supercomplex in Arabidopsis during state transitions. *Biochim. Biophys. Acta* **1847**, 1539–1548 (2015).
44. X. Pan *et al*., Structure of the maize photosystem I supercomplex with light-harvesting complexes I and II. *Science* **360**, 1109–1113 (2018).
45. J. M. Anderson, P. Horton, E.-H. Kim, W. S. Chow, Towards elucidation of dynamic structural changes of plant thylakoid architecture. *Philos. Trans. R. Soc. Lond. B Biol. Sci.* **367**, 3515–3524 (2012).
46. A. S. Verhoeven, A. Kertho, M. Nguyen, Characterization of light-dependent regulation of state transitions in gymnosperms. *Tree Physiol.* **36**, 325–334 (2016).
47. E. Roitinger *et al*., Quantitative phosphoproteomics of the ataxia telangiectasia-mutated (ATM) and ataxia telangiectasia-mutated and rad3-related (ATR) dependent DNA damage response in *Arabidopsis thaliana*. *Mol. Cell. Proteomics* **14**, 556–571 (2015).
48. X. P. Li *et al*., A pigment-binding protein essential for regulation of photosynthetic light harvesting. *Nature* **403**, 391–395 (2000).
49. C. Gerotto, C. Franchin, G. Arrigoni, T. Morosinotto, In vivo identification of photosystem II light harvesting complexes interacting with PHOTOSYSTEM II SUBUNIT S. *Plant Physiol.* **168**, 1747–1761 (2015).
50. V. Correa-Galvis, G. Poschmann, M. Melzer, K. Stühler, P. Jahns, PsbS interactions involved in the activation of energy dissipation in Arabidopsis. *Nat. Plants* **2**, 15225 (2016).
51. J. Sacharz, V. Giovagnetti, P. Ungerer, G. Mastroianni, A. V. Ruban, The xanthophyll cycle affects reversible interactions between PsbS and light-harvesting complex II to control non-photochemical quenching. *Nat. Plants* **3**, 16225 (2017).
52. P. Horton *et al*., Control of the light-harvesting function of chloroplast membranes by aggregation of the LHCII chlorophyll-protein complex. *FEBS Lett.* **292**, 1–4 (1991).
53. P. Horton, M. Wentworth, A. Ruban, Control of the light harvesting function of chloroplast membranes: The LHCII-aggregation model for non-photochemical quenching. *FEBS Lett.* **579**, 4201–4206 (2005).
54. M. P. Johnson *et al*., Photoprotective energy dissipation involves the reorganization of photosystem II light-harvesting complexes in the grana membranes of spinach chloroplasts. *Plant Cell* **23**, 1468–1479 (2011).
55. M. A. Ware, V. Giovagnetti, E. Belgio, A. V. Ruban, PsbS protein modulates non-photochemical chlorophyll fluorescence quenching in membranes depleted of photosystems. *J. Photochem. Photobiol. B* **152**, 301–307 (2015).
56. A. Porcar-Castell, A high-resolution portrait of the annual dynamics of photochemical and non-photochemical quenching in needles of Pinus sylvestris. *Physiol. Plant.* **143**, 139–153 (2011).
57. E. M. Aro, S. McCaffery, J. M. Anderson, Photoinhibition and D1 protein degradation in peas acclimated to different growth irradiances. *Plant Physiol.* **103**, 835–843 (1993).
58. R. J. Porra, W. A. Thompson, P. E. Kriedemann, Determination of accurate extinction coefficients and simultaneous-equations for assaying chlorophyll-a and chlorophyll-B extracted with 4 different solvents—Verification of the concentration of chlorophyll standards by atomic-absorption spectroscopy. *Biochim. Biophys. Acta Bioenerg.* **975**, 384–394 (1989).
59. Y. Perez-Riverol *et al*., The PRIDE database and related tools and resources in 2019: Improving support for quantification data. *Nucleic Acids Res.* **47**, D442–D450 (2019).